

Impurity and band effects competition on the appearance of Inverse Giant Magnetoresistance in Cu/Fe multilayers with Cr

J. Milano* and A.M. Llois

*Departamento de Física, Comisión Nacional de Energía Atómica. Av. Gral. Paz 1499 - (1650) San Martín, Argentina. and
Departamento de Física “Juan José Giambiagi”,
Facultad de Ciencias Exactas y Naturales, Universidad de Buenos Aires. Pabellón I,
Ciudad Universitaria - (1429) Buenos Aires, Argentina.*

L.B. Steren

*Centro Atómico Bariloche and Instituto Balseiro. (8400) S.C. de Bariloche, Argentina
(Dated: October 27, 2018)*

We have studied the dependence of impurity *vs.* band effects in the appearance of inverse giant magnetoresistance (IGMR) in Cu/Fe superlattices with Cr. Current in plane (CIP) and current perpendicular to the plane (CPP) geometries are considered. For the calculation of the conductivities we have used the linearized Boltzmann equation in the relaxation time approximation. Cr impurity effects are taken into account through the spin dependent relaxation times and the band effects through the semiclassical velocities obtained from the LDA calculated electronic structure. The larger the Cr/Fe hybridization strength, the bigger is the tendency towards IGMR. In particular, in CIP geometry roughness at these interfaces increases the IGMR range. The results are compared with experiments and we conclude that the experimental GMR curves can only be explained if Cr bands are present.

PACS numbers: 75.70.Pa, 73.21.Ac, 71.15.Ap

I. INTRODUCTION

The fast development of new materials and their applications to nanodevices have made of transport properties a hot area of research in the last years. Many of these nanodevices are based on magnetic multilayers (MMLs), which show the Giant Magnetoresistance effect (GMR) discovered in 1988¹, that has produced a big impact because of the novel physics responsible of the mechanisms involved in this phenomenon.

Due to the nanolength scales that are reached by new devices, transport may show up in two possible regimes: diffusive for length scales larger than the mean free path, or ballistic if they are shorter. Actually, in a real MML there could certainly exist an interplay between both regimes.

The spin-dependent potential seen by the electrons in these nanosystems is responsible for GMR and this potential can be classified as being of two types. One of them is the so-called extrinsic potential given by scattering with defects in the bulk and at interfaces and it is usually assumed to be the main source of GMR in the diffusive regime. The other type of spin-dependent potential, the intrinsic one, is determined by potential steps at the ideal interfaces of the MMLs. If the system is considered periodic, all information about the intrinsic potential is given by the energy bands. Schep *et al.* in Ref. 2 show that GMR in the ballistic regime is produced by the intrinsic potential. However, calculations done within the semiclassical approach, using the Boltzmann equation in the relaxation time approximation, have accounted for several experimental results in the diffusive regime^{3,4,5}.

The experiments on magnetotransport in MMLs are mostly performed with the electric current flowing parallel to the interfaces (CIP geometry) because the experimental setup in this geometry is easier to achieve than the one corresponding to the current flowing perpendicular to the interfaces (CPP). But the CPP transport configuration is theoretically easier to understand and to modelise⁶. In CIP geometry the electric transport is always diffusive because in this geometry the lengths travelled by the electrons are much larger than the mean free path. In CPP it is possible to obtain length scales larger, of the same order, or shorter than the mean free path. Thereafter in this last geometry, diffusive, ballistic or an interplay between these regimes can be present or achievable. But, questions concerning the relative importance of different factors on GMR such as (a) interfacial roughness and/or interdiffusion⁷, (b) competition among the different length scales⁸ and of (c) bulk *vs.* interfacial scattering^{9,10} are still open and are being actively investigated.

One of the most successful and frequently used transport models for MMLs is the Valet-Fert's¹¹ one (V-F). This simple model is specially well suited for diffusive transport in CPP configuration. The main idea behind this description is that electric transport in a MML can be modelised assuming that there are two currents, a minority and a majority one contributing both independently to the total current, and also that each layer of a MML is thick enough to be considered as a resistor. The MMLs can be regarded as being built by resistors arranged in series, each resistor being a source of scattering (in the bulk or at interfaces). For this assumption to be valid there should be no quantum interference among

sources of scattering. If the distance between interfaces is shorter than the mean free path there will be quantum coherence and this model breaks down (Bozec *et al.*⁸). Actually the V-F model has been successfully applied even on systems that are far beyond the formal validity limits. But, nowadays it is possible to grow MMLs composed of very thin layers and due to this fact the different components of these MMLs cannot be treated as independent resistors and should be treated as a whole^{3,4,5}.

In CPP the characteristic length for transport is the spin diffusion one. In general, the spin diffusion length is larger than the mean free path or coherence length. Coherence lengths in MMLs are of the order of layers' thicknesses due to roughness and spin accumulation at interfaces. In CIP there is no spin accumulation and the electrons traverse a fewer number of interfaces than in CPP, this means that if the thickness of the layers in the multilayers is less than the mean free path (the coherence limit) a transport model based on band structure calculations becomes realistic in the dilute impurity limit.

Experimentally two kinds of GMR can be observed: direct and inverse. In the first case the resistance decreases and in the second one it increases with the applied magnetic field. Direct GMR (DGMR) is more commonly observed than the inverse one (IGMR), which has only been measured in a few systems^{12,13,14}. In particular, George *et al.*¹² found a small IGMR ratio for transport in the CIP configuration for a Cu/Fe multilayer system when a thin Cr layer is intercalated in half of the Fe layers. This inverse effect has been attributed to the existence of alternating spin asymmetries in the samples, due to different coefficients of the spin-dependent scattering of electrons at the different interfaces of the superlattice¹⁵ (this explanation is actually better suited for measurements done in CPP geometry). In this experiment, a mixing of low field IGMR, which adds to the high field normal DGMR to be attributed to Cr/Fe, is observed. At low field (<150 G) the IGMR is due to the alternating spin asymmetries of the two different kinds of magnetic layers present in the sample. For larger fields, the normal and large DGMR usually observed in Cr/Fe multilayers overweights the low field effect until for very large fields the Fe spins within the Fe/Cr/Fe trilayers finally align.

In this contribution we want to investigate the differences between the two kinds of transport geometries and also to get insight into the relative importance of band and impurity effects in the determination of the GMR ratio, in particular for multilayer systems of the type (Fe/Cu/Fe/Cr/Fe/Cu)_N, which we consider are ideal for this study. We mainly calculate low field GMR ratios, that is the GMR ratios which correspond to saturation fields for the relatively weak AF coupling in Cu/Fe multilayers¹⁶.

The questions we want to address are: (a) the relative importance of intrinsic (bands) *vs.* extrinsic potential (impurities) effects on the observed IGMR in Cu/Fe MMLs containing Cr, (b) the dependence of the GMR ratio on the number of Cr/Fe interfaces and/or on the

roughness of the interfaces, and (c) the possible coexistence of IGMR in one geometry and DGMR in the other. To carry out this study we consider Cu/Fe multilayers in which one or more layers of Cr atoms are intercalated in the middle of alternating Fe layers. As Fe and Cr have nearly the same atomic volume one expects Cr to partially interdiffuse. We also think that depending on growth conditions interdiffusion is not necessarily complete; it should, thus, be possible to consider that, in the average, a continuous Cr layer survives leading the Cr band effects and that interdiffused atoms can be regarded as impurities. We compare, then, results of GMR calculations for different interfacial arrangements of Fe and Cr atoms in the above mentioned MMLs and analyse the different contributions leading to IGMR in these MMLs.

The band contribution on transport is explicitly taken into account through the Boltzmann semiclassical approach within the relaxation time approximation. The relaxation time value is considered to be due to impurity scattering at interfaces and in the bulk. The goal is to "measure" the relative importance of having ordered Cr/Fe interfaces *vs.* Cr impurities on the sign of the GMR of these systems. The influence of the number of Cr/Fe interfaces is investigated as well as the effect of having an ordered alloy (roughness) at the interfaces. The GMR is calculated as a function of the relative concentration of Cu and Cr scatterers which constitute the impurity effect. This paper is organized as follows: After this introduction the method of calculation is outlined in Sec. II, while the results are provided in Sec. III. and concluding in Sec. IV.

II. METHOD OF CALCULATION

The electronic structure of the considered superlattices is obtained using an all-electron *ab initio* method. The calculations are performed using the WIEN97 code¹⁷, which is an implementation of the linearized augmented plane wave method (FP-LAPW), based on Density Functional Theory. The local spin density approximation (LSDA) for the exchange and correlation energy as given by Perdew and Wang is used¹⁸.

The conductivities are calculated within the Boltzmann approach in the relaxation time approximation and no spin-flip scattering is considered. The semiclassical Boltzmann equation is valid only in the low impurity limit. The conductivity tensor is given, then, by¹⁹

$$\sigma_{ij} = \frac{e^2}{8\pi^2} \sum_{\nu s} \tau^s \int v_{i\nu}^s(\mathbf{k}) v_{j\nu}^s(\mathbf{k}) \delta[\varepsilon_{\nu}^s(\mathbf{k}) - \varepsilon_F] d^3\mathbf{k}, \quad (1)$$

s denotes spin index, ν the band index, ε_F is the Fermi energy. The semiclassical velocities $v_{j\nu}^s(\mathbf{k})$ are obtained from the band calculations. The relaxation time, τ^s , is \mathbf{k} state independent but spin dependent within our model.

Following Ref. 5, for the determination of τ^s we assume that the local spin densities of state at the Fermi level in the magnetic layers of the superlattice have all the same value. We also assume that there are interdiffused Cu impurities in the Cu/Fe interfaces and Cr impurities in the Cr/Fe ones as well. It was shown, in Ref. 20, that magnetic impurities in Cu make a small contribution to the local density of states at the Fermi level, and should be, thereafter, ineffective for GMR. As the Boltzmann approximation is valid only in the low impurity limit, we assume that the concentration of both types of scatterers (c_{Cr} and c_{Cu}) is very small.

We are interested in the evolution of GMR as a function of the relative importance of both types of scatterers through their modification of τ^s . Thus, we assume that for each of the studied superlattices, the total number of scatterers per unit cell is fixed and it is equal to a certain constant, K , that is

$$c_{Cr} N_{Cr/Fe} + c_{Cu} N_{Cu/Fe} = K \quad c_{Cu}, c_{Cr} \ll 1, \quad (2)$$

$N_{A/Fe}$ is the number of A/Fe interfaces per unit cell (A = Cr or Cu) and c_A the atomic concentration of atoms of type A at the corresponding interfaces. We propose the following expression for the relaxation time averaged over the Fermi surface,

$$\frac{1}{\tau^s} = \frac{K}{N} \left(\frac{1 - \bar{x}_{Cr}}{\tau_{Cu/Fe}^s} + \frac{\bar{x}_{Cr}}{\tau_{Cr/Fe}^s} \right), \quad (3)$$

where

$$\bar{x}_{Cr} = \frac{N_{Cr/Fe} c_{Cr}}{N_{Cu/Fe} c_{Cu} + N_{Cr/Fe} c_{Cr}}$$

and

$$N = N_{Cr/Fe} + N_{Cu/Fe}.$$

\bar{x}_{Cr} is then the Cr relative scatterer concentration. $\tau_{A/Fe}$ denotes the relaxation time of Fe in the presence of A type impurities (A=Cr, Cu). When calculating the GMR ratios the factor K/N in Eq. (3) cancels out.

For the antiparallel configuration the corresponding expression for τ^s , which mixes local majority and minority relaxation times in subsequent Fe layers has to be considered.

In our calculations we obtain the values of $\tau_{A/Fe}^s$ appearing in expression (3) from the spin asymmetries, $\beta_{A/Fe} = \tau_{A/Fe}^\uparrow / \tau_{A/Fe}^\downarrow$, as given in Ref. 5, and from

$$\sigma_{A/Fe} = \tau_{A/Fe}^\uparrow \tilde{\sigma}_{Fe}^\uparrow + \tau_{A/Fe}^\downarrow \tilde{\sigma}_{Fe}^\downarrow, \quad (4)$$

where $\tilde{\sigma}_{Fe}^s$ are the isotropic band contributions to Fe bulk conduction for the corresponding spin channel divided by its relaxation time. $\tilde{\sigma}_{Fe}^s$ are obtained from our electronic bands calculations. $\sigma_{A/Fe}$ is the inverse of the total residual resistivity of bulk Fe in the presence of 1% A type

impurities, the corresponding values are taken from Ref. 21. See Table I.

We define the GMR coefficient as

$$\text{GMR} = \frac{\sigma_{ii}(AP)}{\sigma_{ii}(P)} - 1 \quad -1 < \text{GMR} < +\infty \quad (5)$$

where P (AP) stands for parallel (antiparallel) configuration. If this coefficient is positive (negative) we are in the presence of IGMR (DGMR). The P configuration meant in Eq. (5) is the one corresponding to the Fe layers aligned across Cu (low field saturation). AP indicates the initial configuration when the Fe magnetic layers separated by Cu are antiferromagnetically aligned.

III. RESULTS

The calculations have been done for superlattices grown along the (001) direction and following the BCC structure of Fe. As the layers are thin we assume that Cu grows epitaxially on Fe and within the same structure; this is actually being revealed by x-ray spectroscopy²². The calculations are done for superlattices of the type Fe/Cu/(Fe,Cr)/Cu, using a varying number of Cu planes and several combinations of planes and atoms in the (Fe,Cr) region. The in-plane lattice parameter considered is the one corresponding to the LDA optimised Fe buffer, the interface distances Cu/Fe and Cr/Fe are also optimized. The considered muffin tin radius R_{mt} are equal to 2.0 atomic units for the three kinds of atoms involved in the studied systems. The cutoff parameter, that gives the number of plane waves in the interstitial region, is taken as $R_{mt}K_{max}=8$, where K_{max} is the maximum value of the reciprocal lattice vector used in the expansion of plane waves in that zone. We find that the optimized interlayer distance between Fe and Cu layers increases by 5% with respect to LDA bulk Fe while the Fe/Cr interfaces relax by about 4%.

The band structure is calculated using a mesh of 167 \mathbf{k} points in the full Brillouin zone (FBZ) and the band contribution to σ_{ij} in Eq. (1), is obtained using a mesh of 20000 \mathbf{k} points in FBZ. In order to obtain the relative importance of band and impurity effects and the dependence of IGMR on the number of Cr/Fe interfaces on roughness and on geometry (CIP/PPP), we analyse the following situations: 1. Cr band effects on GMR, 2. Cr and Cu impurity effects on the GMR of Fe_N/Cu_M superlattices, 3. Cr and Cu impurities together with Cr band effects.

1. Cr band effects on GMR.

In order to obtain the band contribution of Cr on the GMR ratio we do calculations for a $Fe_3/Cu_4/Fe/Cr/Fe/Cu_4$ superlattice as a function of Cr/Fe interface distance. We certainly know that the ground state for the number of Cu layers considered here is not AP, and that in fact the maximum AP exchange

coupling appears for 8 or 9 layers of Cu. In spite of this, the tendencies we are looking for can be drawn from these calculations which are less demanding in CPU time.

In Fig. 1 we give the results obtained for CPP and CIP-GMR coefficients. The results given in this figure do not take into account the variation of τ^s with impurity concentration, only the band effects on the GMR of this system are considered by taking τ^s to be the same for both spin channels. For comparison we also give the GMR values for the superlattice Fe_3/Cu_4 in Fig. 1(a). Comparing Fig. 1(a) and Fig. 1(b) it can be seen that the modification of the superlattice bands through the introduction of a Cr monolayer gives rise to a large variation of the GMR values, specially in CPP geometry. In Fig. 1(b) the interfacial Cr/Fe distance is equal to the one corresponding to bulk Fe. Fig. 1(c) corresponds to a decrease of 6% in the Cr/Fe interfacial distance, and Fig. 1(d) to a reduction of 10% with respect to Fig. 1(b). It can be seen that increasing the hybridization between Fe and Cr atoms, the tendency towards IGMR also increases. The largest tendencies towards IGMR when introducing a Cr monolayer and when increasing the hybridization are clearly observed in CPP geometry.

2. Cr and Cu impurity effects on Fe_N/Cu_M superlattices.

In this case Cu and Cr scatterers in the dilute impurity limit are introduced in MMLs Fe_N/Cu_M ($N=3, 5$ and $M=4, 8$) through the values of τ^s . No Cr band effects are present, that is no continuous or discontinuous Cr layer is considered, and only the contribution of varying the relative Cr scatterer concentration, \bar{x}_{Cr} , in the low impurity limit on GMR is analysed for several examples. In Fig. 2 we show the result of changing the number of Cu or Fe layers as a function of relative Cr *vs.* Cu impurity concentration for superlattices which do not contain complete or quasicomplete layers of Cr. Only the tendencies are relevant for this discussion. It is useful to remember that negative values mean direct GMR. Changing the number of Fe layers does not modify either the tendencies nor the absolute values of the coefficients. This can be seen by comparing Fig. 2(a) and 2(b) where we increase the number of Fe monolayers from three to five in the superlattices. A tendency towards inverse GMR when increasing \bar{x}_{Cr} can be observed. CPP-GMR is more direct than CIP-GMR for almost all values of \bar{x}_{Cr} , but within this approximation both of them remain direct. Increasing the number of Cu layers increases the tendency of CIP-GMR towards IGMR and it even goes positive within a small range of \bar{x}_{Cr} values (see Fig. 2(c)), which is what is experimentally observed for the Cu width considered. The general tendencies remain the same as in the previous cases. The CPP-GMR ratio remains direct and almost constant with \bar{x}_{Cr} in all the cases studied in Fig. 2.

In the transport calculations performed for this item the Fermi level, ε_F has been kept fixed and equal to its self-consistent value in the corresponding impurity free

multilayer. We have made an estimation of the error done when calculating the GMR ratio while keeping ε_F fixed for the Fe_3/Cu_4 superlattice. In this estimation, we consider that the concentration of Cu and Cr impurities in Fe lies around 5%, which is a large value for the low impurity limit assumed here. For $\bar{x}_{\text{Cr}}=0.5$ the variation in the CPP-GMR ratio due to the Fermi level shift is of 4% and of 2% in CIP, this does not change the observed tendencies. We consider that for the other cases here treated the situation is similar to the present one.

3. Cr and Cu impurity effects and Cr band effects.

We analyse in the following examples Cr band effects and, simultaneously, Cr and Cu impurity effects on the GMR ratios of the studied superlattices. Cr band effects are taken into account by introducing continuous and discontinuous Cr layers, and the impurity effects through the variation of τ^s as a function of relative impurity concentration in the low impurity limit as in the previous examples. It is well known that Cr mixes with Fe, but a certain averaged ordered Cr configuration should survive after deposition.

In Fig. 3 we show the effect on the GMR of introducing a varying number of Cr/Fe interfaces, and also that of including more Cu layers as a function of \bar{x}_{Cr} . We also give the values of GMR when no impurity effects are taken into account (horizontal lines). We see in Fig. 3(a) that the inclusion of Cr band effects through the presence of one Cr layer in the unit cell, drastically modifies CPP-GMR as compared to the results for Fig. 2(a). In the new situation, CPP-GMR goes positive for almost all values of \bar{x}_{Cr} . It should be noticed that Cu impurities lower the GMR coefficient if one compares with the results of calculations that only include band effects (straight lines in Fig. 3). An increase in \bar{x}_{Cr} drives both GMR coefficients positive.

If one changes the number of Cu layers, CPP-GMR goes down even if it is mostly positive, but CIP-GMR remains nearly unaffected; see Fig. 3(b). We expect that in the real situation, with the number of Cu layers lying around 8-9 for the maximum antiferromagnetic coupling, CPP-GMR should be inverse and larger than CIP-GMR. On the other hand, CIP-GMR is nearly not modified when the number of Cu layers is changed within the widths we are treating in these calculations.

Duplicating the number of Cr/Fe interfaces does not give rise to a significant change in CIP-GMR while CPP-GMR nearly doubles its value, as it is shown in Fig. 3(c).

We simulate a particular case of roughness by adding an ordered 50% Cr and 50% Fe ML on each side of the Cr layer (see Fig. 3(d)), and we obtain a larger \bar{x}_{Cr} range for which CIP-GMR is inverse, while CPP-GMR does not change with respect to the example of Fig 3(a). This can be easily understood as the introduction of roughness generates Cr/Fe interfaces perpendicular to the superlattice growth direction, and we have already seen that the presence of these interfaces is a source of inverse GMR

due to Cr/Fe hybridization. The effect is nevertheless not large enough as to qualitatively modify the maximum value reached by the GMR ratio. CPP-GMR does not change in this particular example as the number of Cr/Fe interfaces along z is the same as in the example of Fig. 3(a). It is interesting to notice that GMR has a maximum as a function of concentration in each one of the studied cases.

We also simulate the effect of applying large magnetic fields to the samples, that is, the process of aligning not only the magnetic moments of Fe across Cu, but also those of Cr with respect to the adjacent Fe atoms. In our calculations we observe that Cr has a tendency to antiferromagnetically align with respect to the surrounding Fe layers both in the AP configuration as in the P configuration. To simulate the presence of the external magnetic field, we do fixed spin moment calculations by constraining the total cell magnetic moment and increasing it progressively towards its high field saturation value. In Table II we show the results obtained for the example $\text{Fe}_3/\text{Cu}_4/\text{Fe}/\text{Cr}/\text{Fe}/\text{Cu}_4$ and $\bar{x}_{\text{Cr}}=0.5$. We give the obtained GMR ratios for different values of the total magnetic moment, together with the local magnetic moments on Cr and on the neighboring Fe atoms for each constrained total magnetic moment. The experimental behavior for the evolution of GMR in the presence of growing magnetic fields is obtained. That is, an initial increase in the values of the GMR ratios until the low saturation limit is reached and beyond this, a slow decrease in the GMR ratios as a function of growing applied magnetic field¹². This shows again the importance of band effects on the GMR of the system under study, as this evolution of GMR would not have been observed if only impurity effects had been taken into account.

IV. CONCLUSIONS

Based on *ab initio* band structure calculations, we try to determine the competition between Cr band and impurity effects on the type of GMR (direct or inverse) for superlattices of the type $(\text{Fe}/\text{Cu}/\text{Fe}/\text{Cr}/\text{Fe}/\text{Cu})_N$. The conductivities used to obtain the GMR ratios are calculated semiclassically by using the linearized Boltzmann approach. The impurity effects are taken into account through an averaged relaxation time per spin channel. We make calculations for, both, CIP and CPP geometries and work in the low impurity limit. The conclusions drawn can be summarized as follows:

The value and sign of GMR depends strongly on the hybridization strength between Fe and Cr layers, specially in CPP geometry.

In the absence of Cr band effects and when only isolated Cr and Cu impurities in Fe are considered,

Fe_N/Cu_M superlattices show a clear tendency towards IGMR in CIP configuration. This tendency depends on the relative concentration of Cr *vs.* Cu impurities. For some Cu widths and within a certain concentration range it even goes positive. In CPP the situation is different, the GMR ratio is far from being inverse over the whole range of relative impurity concentrations. These results had already been observed by P. Zahn *et al.*⁵. A change in the number of Fe layers does not modify these tendencies.

When complete or incomplete Cr layers are introduced in alternating Fe layers and, thereafter, Cr band effects are switched on, quantitative as qualitative changes take place specially in CPP. Both, in CIP as CPP the GMR ratios acquire a larger tendency towards IGMR, but in this case it is the CPP geometry the one with the largest IGMR ratios. In the two geometries the GMR is inverse within a broad range of the Cr and Cu relative impurity concentration. In CPP, Cr/Fe interface effects are more important than impurity ones to determine the type of GMR, while the opposite is true in CIP. This is being confirmed by the fact that doubling the number of Fe/Cr interfaces (see Fig 3) gives rise to a large increase in CPP-IGMR, while the increment in CIP-GMR is not as important.

The introduction of roughness (in our case an ordered roughness) at the interfaces, gives rise to an increasing tendency towards CIP-IGMR. Electrons flowing in CIP geometry face the appearance of effective Cr/Fe interfaces in the presence of roughness and Cr band effects become more relevant in this geometry.

We have shown that the experimentally observed evolution of GMR for Fe_N/Cu_M MMLs with Cr, as a function of an increasing external magnetic field, can be explained if the presence of Cr bands is assumed.

In general, both transport geometries share the same tendencies for the sign of the GMR ratio, even if the presence of Cr band effects makes CPP more liable to IGMR than CIP, contrary to what happens when only Cr impurities are considered.

Summarizing, both disorder as band effects are necessary to explain the appearance and evolution of IGMR in the studied superlattices.

Acknowledgments

We thank Dr. M. Alouani for helpful and fruitful discussions. Two of us (A.M.L. and L.B.S.) acknowledge Consejo Nacional de Investigaciones Científicas y Técnicas for support of this work. We acknowledge Fundación Sauberan, Fundación Antorchas and Fundación Balseiro also for support. This work was partially funded by project UBACyT X115.

* Electronic address: milano@cnea.gov.ar

¹ M.N. Baibich, J.M. Broto, A. Fert, F. Nguyen Van Dau, F.

- Petroff, P. Etienne, G. Creuzet, A. Friederich, J. Chazelas, Phys. Rev. Lett. **61**, 2472 (1988).
- ² K.M. Schep, P.J. Kelly, G.E.W. Bauer, Phys. Rev. Lett. **74**, 586 (1995).
- ³ M. Weissmann, A.M. Llois, R. Ramírez, M. Kiwi, Phys. Rev. B **54**, 15335 (1996).
- ⁴ R. Gómez Abal, A.M. Llois, M. Weissmann, Phys. Rev. B **53**, R8844 (1996).
- ⁵ P. Zahn, I. Mertig, M. Richter, and H. Eschrig, Phys. Rev. Lett. **75**, 2996 (1995).
- ⁶ M.A.M. Gijs, G.E.W. Bauer, Adv. Phys. **46**, 285 (1997).
- ⁷ M.C. Cyrille, S. Kim, M.E. Gomez, J. Santamaria, K.M. Krishnan, I.K. Schuller, Phys. Rev. B **62**, 3361 (2000).
- ⁸ D. Bozec, M.A. Howson, B.J. Hickey, S. Shatz, N. Wisser, E.Y. Tsymbal, D.G. Pettifor, Phys. Rev. Lett. **85**, 1314 (2000).
- ⁹ J. Santamaria, M.E. Gomez, M.C. Cyrille, C. Leighton, K.M. Krishnan, I.K. Schuller, Phys. Rev. B **65**, 012412-1 (2001).
- ¹⁰ C. Vouille, A. Barthélémy, F. Elokun Mpondo, A. Fert, P.A. Schroeder, S.Y. Hsu, A. Reilly, R. Loloee, Phys. Rev. B **60**, 6710 (1999).
- ¹¹ T. Valet, and A. Fert, Phys. Rev. B **48**, 7099 (1993).
- ¹² J.M. George, L.G. Pereira, A. Barthélémy, F. Petroff, L. Steren, J.L. Duvail, A. Fert, R. Loloee, P. Holody, P.A. Schroeder, Phys. Rev. Lett. **72**, 408 (1994).
- ¹³ J.-P. Renard, P. Bruno, R. Mégy, B. Bartenlian, P. Beauvillain, C. Chappert, C. Dupas, E. Kolb, M. Mulloy, P. Veillet, E. Vélú, Phys. Rev. B **51**, 12821 (1995).
- ¹⁴ K. Rahmouni, A. Dinia, D. Stoeffler, K. Ounadjela, H.A.M. Van den Berg, H. Rakoto, Phys. Rev. B **59**, 9475 (1999).
- ¹⁵ A. Fert, I.A. Campbell, J. Phys. F **6**, 849 (1976).
- ¹⁶ F. Petroff, A. Barthélémy, D.H. Mosca, D.K. Lottis, A. Fert, P.A. Schroeder, W.P. Pratt, Jr., R. Loloee, S. Lequien, Phys. Rev B **44**, 5355, (1991).
- ¹⁷ P. Blaha, K. Schwarz, J. Luitz, WIEN97, Vienna University of Technology, Vienna 1997. (Improved and updated Unix version of the original copyrighted WIEN-code, which was published by P. Blaha, K. Schwarz, P. Sorantin, S. B. Trickey, in Comput. Phys. Commun. **59**, 399 (1990).
- ¹⁸ J.P. Perdew, Y. Wang, Phys. Rev. B **45**, 13244 (1992).
- ¹⁹ J.M. Ziman, *Electrons and Phonons* (Oxford University Press, London, 1967), Chap. VII.
- ²⁰ P. Zahn, J. Binder, I. Mertig, R. Zeller, P.H. Dederichs, Phys. Rev. Lett. **80**, 4309 (1998).
- ²¹ I. Mertig, P. Zahn, M. Richter, H. Eschrig, R. Zeller, and P.H. Dederichs, J. Magn. Magn. Mater. **151**, 363 (1995).
- ²² S. Pizzini, F. Baudelet, D. Chandessris, A. Fontaine, H. Magnan, J.M. George, F. Petroff, A. Barthélémy, A. Fert, R. Loloee, P.A. Schroeder, Phys. Rev. B **46**, 1253 (1992).

	Impurity (A)	
	Cr	Cu
$\sigma_{A/Fe}^{\uparrow}$	0.12	0.53
$\sigma_{A/Fe}^{\downarrow}$	0.70	0.065
$\beta_{A/Fe}$	0.11	3.68
$\tau_{A/Fe}^{\uparrow}$	1.05	4.84
$\tau_{A/Fe}^{\downarrow}$	9.75	1.31

TABLE I: $\sigma_{A/Fe}^s$ is the inverse of the residual resistivity of Fe bulk in the presence of A-type impurities (1%); the values are taken from Ref. 21 and are given in $(\mu\Omega.cm)^{-1}$. $\beta_{A/Fe}$ means the asymmetry coefficient of Fe in the presence of A-type impurities; the values are taken from Ref. 5. $\tau_{A/Fe}^s$ are the Fe relaxation times per spin channel obtained using Eq. (4) and are given in arbitrary units.

Magnetic configuration					
	μ_{cell}	μ_{Fe}	μ_{Cr}	CIP-GMR	CPP-GMR
AP	-4.88	1.14	-0.22	0	0
P	8.82	1.02	-0.25	0.12	0.65
FSM1	13.00	1.95	0.30	-0.20	0.27
FSM2	16.00	2.42	0.98	-0.30	-0.34

TABLE II: CIP and CPP-GMR coefficients calculated for different initial magnetic configurations of the superlattice $Fe_3/Cu_4/Fe/Cr/Fe/Cu_4$. μ_{cell} denotes the total magnetic moment per unit cell and μ_A the local magnetic moments on Cr or on the Fe atoms adjacent to the Cr layer. AP denotes the initial zero field magnetic configuration, P means the low field saturation configuration (Fe layers aligned across Cu), FSM1 and FSM2 stand for configurations in which the total magnetic moment is larger than for the P one. All moments are given in units of μ_B .

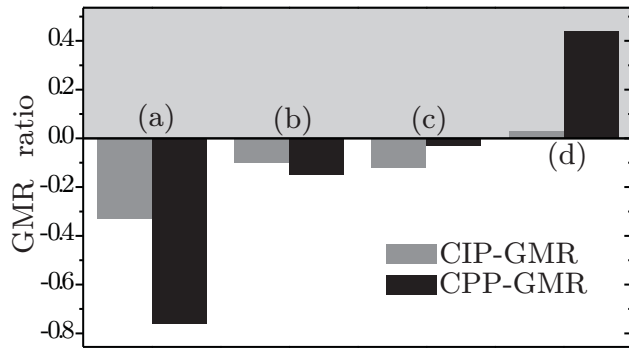


FIG. 1: Calculated GMR for a) Fe_3/Cu_4 , b) $\text{Fe}_3/\text{Cu}_4/\text{Fe}/\text{Cr}/\text{Fe}/\text{Cu}_4$ with interfacial Cr/Fe distance equal to the one of bulk Fe, c) and d) idem b) but with Cr/Fe distance 6% and 10% respectively smaller. The superlattices are grown along the (001) direction. In this case the in plane lattice parameter are those of Fe bulk.

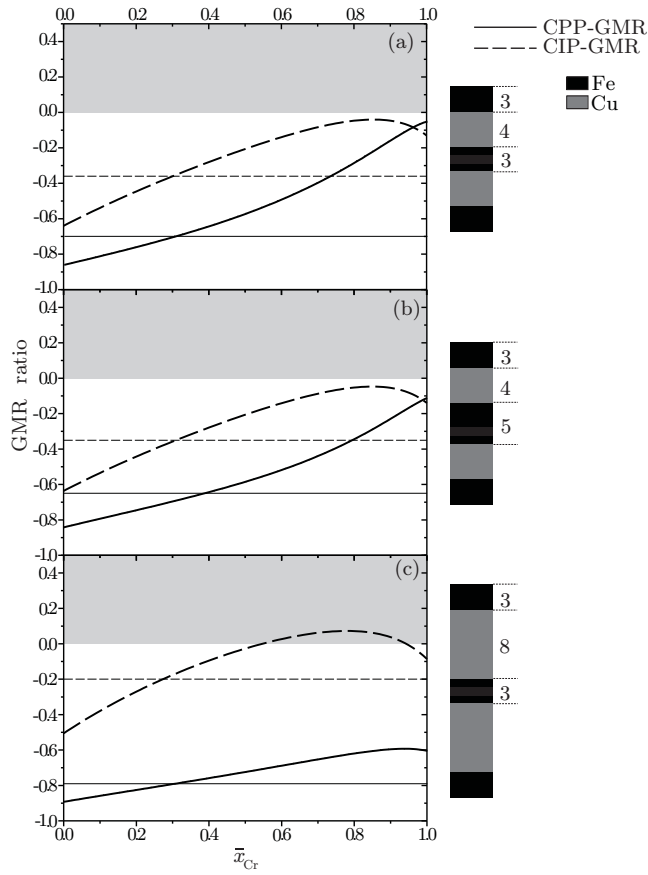


FIG. 2: Calculated GMR for a) Fe_3/Cu_4 , b) Fe_5/Cu_4 and c) Fe_3/Cu_8 as a function of the relative Cr scatterer concentration, \bar{x}_{Cr} . Shaded areas correspond to IGMR. Straight lines give the GMR ratios in the absence of impurity scatterers. No Cr band effects present. The number of atomic layers in each layer of the MMLs is given on the right of the schematic MMLs.

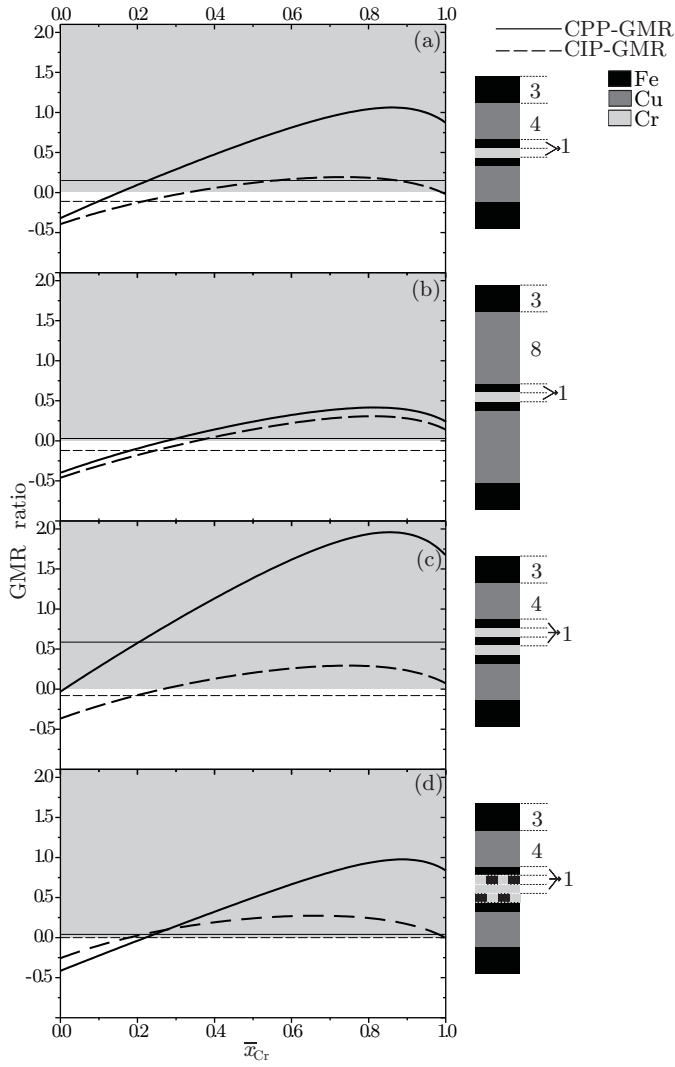


FIG. 3: Calculated GMR for a) Fe₃/Cu₄/Fe/Cr/Fe/Cu₄, b) Fe₃/Cu₈/Fe/Cr/Fe/Cu₈, c) Fe₃/Cu₄/Fe/Cr/Fe/Cr/Fe/Cu₄, d) Fe₃/Cu₄/Fe/Fe_{0.5}Cr_{0.5}/Fe/Fe_{0.5}Cr_{0.5}/Fe/Cu₄ as a function of the relative Cr/Cu scatterer concentration, \bar{x}_{Cr} . Straight lines give the GMR ratios in the absence of impurity scatterers. The number of atomic layers in each layer of the MMLs is given on the right of the schematic MMLs.